

THEORETICAL KINETIC ESTIMATES FOR THE RECOMBINATION OF HYDROGEN ATOMS WITH PROPARGYL AND ALLYL RADICALS

LAWRENCE B. HARDING¹ AND STEPHEN J. KLIPPENSTEIN²

¹*Chemistry Division
Argonne National Laboratory
Argonne, IL 60439, USA*

²*Chemistry Department
Case Western Reserve University
Cleveland, OH 44106-7078, USA*

Ab initio quantum chemical simulations were coupled with variational transition state theory in estimating rate constants for the $\text{H} + \text{C}_3\text{H}_3$ and $\text{H} + \text{C}_3\text{H}_5$ recombination reactions. The energy of interaction between the H atom and each of the radicals was evaluated at the CAS + 1 + 2 level for the range of separations and relative orientations spanning the transition state region. An analytic representation of these interaction energies was then implemented in variable reaction coordinate transition state theory calculations of the high pressure limit recombination rate constant for temperatures ranging from 200 to 2000 K. For the propargyl reaction, the overall addition rate was separated into contributions correlating with the initial formation of allene and propyne. These theoretical results were compared with the available experimental data as well as with corresponding theoretical estimates for the $\text{H} + \text{C}_2\text{H}_3$ and $\text{H} + \text{C}_2\text{H}_5$ reactions. The $\text{H} + \text{propargyl}$ and $\text{H} + \text{allyl}$ total recombination rates were remarkably similar, with both being greater than the $\text{H} + \text{vinyl}$ and $\text{H} + \text{ethyl}$ rates, due to the presence of twice as many addition channels.

Introduction

It has been widely suggested that the relatively high concentrations (in the combustion environment) of resonantly stabilized radicals, such as the propargyl radical, are the result of their comparatively low rates of reaction [1]. In this work we examine the reaction kinetics for the recombination of H atoms with two such resonantly stabilized radicals; the allyl radical (CH_2CHCH_2) and the propargyl radical (CHCCH_2). The allyl radical, with its two degenerate resonance structures, is a prototypical resonantly stabilized radical. The propargyl radical also has two dominant resonance structures, but, unlike allyl, the two structures are not equivalent.

There is considerable recent interest in the rates of propargyl radical reactions due to the postulated role of propargyl radicals in the soot formation process, and particularly the initial formation of benzene [1]. In spite of this interest, the available experimental data for both the $\text{H} + \text{propargyl}$ [2–4] and the $\text{H} + \text{allyl}$ [5] reactions are quite limited. The present coupling of high-level quantum chemical simulations with sophisticated transition state theory evaluations should provide quantitatively meaningful *a priori* estimates for the kinetics of

these two reactions. Comparison with related theoretical results for the $\text{H} + \text{vinyl}$ [6] and $\text{H} + \text{ethyl}$ [7] reactions allows for a reasonably direct examination of the effects of resonance stabilization on the kinetics.

For the propargyl radical there are two distinct addition products, allene (CH_2CCH_2) and propyne (CH_3CCH), formed by attack on different ends of the propargyl radical. For allyl, the only stable addition product is propene (CH_3CHCH_2), which can be formed by attack on either end. Both radicals are planar, and attack can occur from either above or (equivalently) below the plane of the radical. Thus, for allyl there are four distinct pathways, all of which are related by symmetry. For propargyl, there are also four distinct pathways, which can be divided into two symmetry-related pairs, one pair leading to allene and the other to propyne.

Here, the interaction of the H atom with each of the radicals for each of the addition paths is first characterized with high-level *ab initio* quantum chemical simulations. The resulting analytical potentials are then implemented in variable reaction coordinate transition state theory-based estimates for the high-pressure recombination kinetics. The results of these calculations are directly compared with the available experimental data.

Report Documentation Page

Form Approved
OMB No. 0704-0188

Public reporting burden for the collection of information is estimated to average 1 hour per response, including the time for reviewing instructions, searching existing data sources, gathering and maintaining the data needed, and completing and reviewing the collection of information. Send comments regarding this burden estimate or any other aspect of this collection of information, including suggestions for reducing this burden, to Washington Headquarters Services, Directorate for Information Operations and Reports, 1215 Jefferson Davis Highway, Suite 1204, Arlington VA 22202-4302. Respondents should be aware that notwithstanding any other provision of law, no person shall be subject to a penalty for failing to comply with a collection of information if it does not display a currently valid OMB control number.

1. REPORT DATE 04 AUG 2000	2. REPORT TYPE N/A	3. DATES COVERED -			
4. TITLE AND SUBTITLE Theoretical Kinetic Estimates for the Recombination of Hydrogen Atoms with Propargyl and Allyl Radicals.		5a. CONTRACT NUMBER			
		5b. GRANT NUMBER			
		5c. PROGRAM ELEMENT NUMBER			
6. AUTHOR(S)		5d. PROJECT NUMBER			
		5e. TASK NUMBER			
		5f. WORK UNIT NUMBER			
7. PERFORMING ORGANIZATION NAME(S) AND ADDRESS(ES) Chemistry Division Argonne National Laboratory Argonne, IL 60439, USA		8. PERFORMING ORGANIZATION REPORT NUMBER			
9. SPONSORING/MONITORING AGENCY NAME(S) AND ADDRESS(ES)		10. SPONSOR/MONITOR'S ACRONYM(S)			
		11. SPONSOR/MONITOR'S REPORT NUMBER(S)			
12. DISTRIBUTION/AVAILABILITY STATEMENT Approved for public release, distribution unlimited					
13. SUPPLEMENTARY NOTES See also ADM001790, Proceedings of the Combustion Institute, Volume 28. Held in Edinburgh, Scotland on 30 July-4 August 2000.					
14. ABSTRACT					
15. SUBJECT TERMS					
16. SECURITY CLASSIFICATION OF:			17. LIMITATION OF ABSTRACT UU	18. NUMBER OF PAGES 8	19a. NAME OF RESPONSIBLE PERSON
a. REPORT unclassified	b. ABSTRACT unclassified	c. THIS PAGE unclassified			

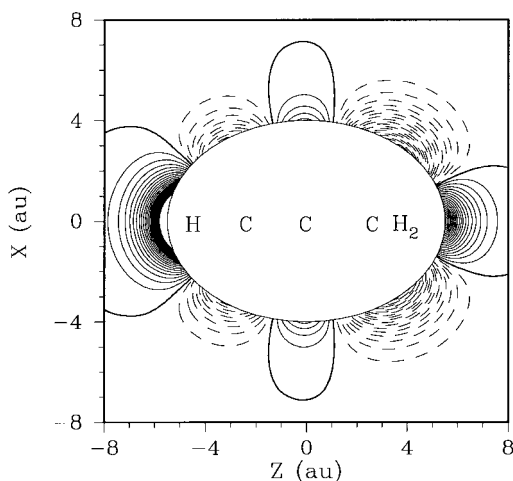


FIG. 1. Two-dimensional cut of the three-dimensional surface for the $\text{H} + \text{C}_3\text{H}_3 \rightarrow \text{C}_3\text{H}_4$ association reaction. The plotting plane is perpendicular to the plane of the C_3H_3 radical and bisects the HCH angle. Solid contours are positive, dashed contours negative, and the zero energy contour (defined to be the energy of the $\text{H} + \text{C}_3\text{H}_3$) is shown with a heavy solid line. The contour increment is 2 kcal/mol, and all distances are shown in atomic units (one atomic unit = 0.52918 Å).

Potential Surface Calculations

Methodology

All the electronic structure results reported here are from multireference configuration interaction (MR-CI) calculations employing orbitals optimized using the complete active space, self-consistent field (CASSCF) methodology. In these calculations, the CASSCF reference wave function consists of four active orbitals (the hydrogen 1s orbital and three π orbitals on the hydrocarbon fragment) and four active electrons. This is the minimum necessary to correctly describe the breaking CH bond and the resonance of the hydrocarbon radical. The effects of higher-order excitations were tested using a multi-reference Davidson correction. The basis set used in most calculations was the correlation-consistent, polarized valence double zeta (cc-pvdz) basis set of Dunning [8–10]. To estimate the error associated with the use of this relatively small basis set, internally contracted, MR-CI calculations were carried out along the association paths for $\text{H} + \text{C}_3\text{H}_3$ using the correlation-consistent, polarized valence triple zeta (cc-pvtz) basis set. The uncontracted CI calculations were carried out using the COLUMBUS package of codes [11]. The internally contracted CI calculations were done using the MOLPRO package [12–16].

Results

Characterization of the potential surface for the association reactions was accomplished by mapping out three-dimensional grids, in polar coordinates, corresponding to motion of the hydrogen atom reactant around the rigid hydrocarbon radicals. These surfaces were fit using techniques described previously in calculations on $\text{H} + \text{C}_2\text{H}_3$ [6] and $\text{H} + \text{C}_2\text{H}_5$ [7].

A two-dimensional slice of the three-dimensional $\text{H} + \text{C}_3\text{H}_3$ surface is shown in Fig. 1. This plot illustrates that association reactions can take place through four barrierless attractive valleys: two symmetry-related paths for attack on the CH end of C_3H_3 , and two for attack on the CH_2 end. Recall that the ground state, electronic wave function of propargyl is an unsymmetrical resonance between a structure having two carbon-carbon double bonds (with the radical orbital on the CH end) and one having one carbon-carbon single bond and one carbon-carbon triple bond (with the radical on the CH_2 end). The C_{2v} equilibrium structure of propargyl implies that the single bond-triple bond structure is the dominant resonance structure. Fig. 1 shows that the paths for attack on the CH_2 side are significantly more attractive and wider (in this in-plane coordinate) than the paths for attack on the CH side; that is, there is, not surprisingly, an energetic preference for attack of the dominant resonance structure. In Fig. 2 we show two perpendicular slices through this potential surface, centered on each of the terminal carbon atoms. From this plot it can be seen that the CH-side paths are somewhat wider in this coordinate than the CH_2 -side paths. This is caused by non-bonded repulsions between the incoming H atom and the two CH bonds on the CH_2 side.

For the $\text{H} + \text{allyl}$ reaction, the calculations show four symmetry-related pathways for barrierless reaction (the hydrogen can attack either terminal carbon from either above or below the plane of the radical). The calculations also predict that approach of the central carbon is repulsive (as was found for $\text{H} + \text{C}_3\text{H}_3$).

To better compare the relative attractiveness of the association paths, we optimized minimum energy paths (MEP) for both $\text{H} + \text{allyl}$ and $\text{H} + \text{propargyl}$. In these calculations the C-H distance was kept fixed at a number of different values, and the two angular coordinates were optimized to find the orientation with the lowest energy (again the geometries of the hydrocarbon radical fragments were kept fixed). Plots of the energy along these MEPs are shown in Fig. 3 along with comparable calculations on $\text{H} + \text{C}_2\text{H}_3$ and $\text{H} + \text{C}_2\text{H}_5$. From this plot it can be seen that the $\text{H} + \text{allyl}$ MEP lies between the two $\text{H} + \text{propargyl}$ MEPs. All of the $\text{H} + \text{resonance stabilized radical}$ MEPs were predicted to be significantly less attractive than the MEPs for the non-resonance stabilized radicals, C_2H_3 and C_2H_5 .

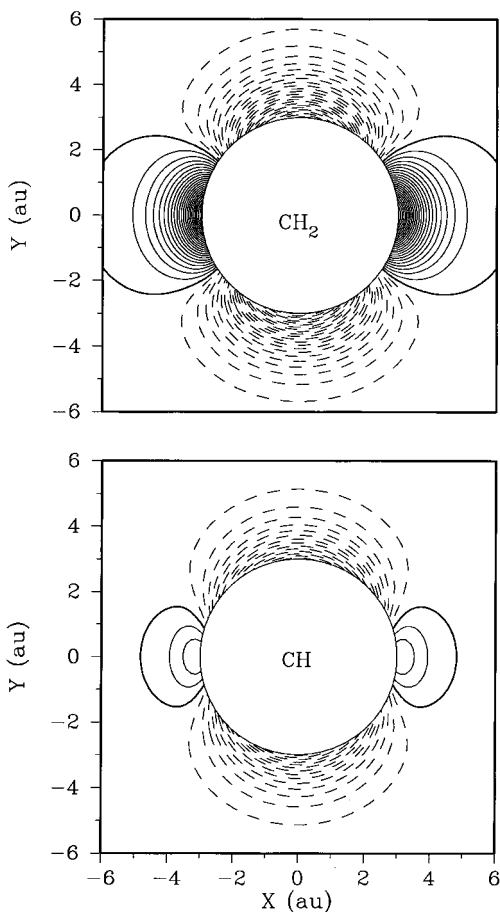


FIG. 2. Two-dimensional cuts of the three-dimensional surface for the $\text{H} + \text{C}_3\text{H}_3 \rightarrow \text{C}_3\text{H}_4$ association reaction. The plotting planes are perpendicular to the CCC axis. The plotting plane for the upper plot contains the CH_2 carbon, while that of the lower plot contains the CH carbon. The other plotting conventions are as in Fig. 1.

The MEPs for the two reactions, $\text{H} + \text{C}_3\text{H}_3 \rightarrow \text{CH}_2\text{CCH}_2$ and $\text{H} + \text{C}_3\text{H}_3 \rightarrow \text{CH}_3\text{CCH}$, were recalculated using the larger cc-pvtz basis set. The cc-pvtz MEPs were found to be slightly more attractive than the cc-pvdz MEPs. The cc-pvdz potential surface was corrected for this deficiency as follows. At each point the distance between the H atom and each of the terminal C atoms was determined. Two corrections were then calculated, one using the difference between the cc-pvdz and cc-pvtz MEPs for addition to the CH_2 end and the distance between the H atom and the CH_2 carbon. The second correction used the difference between the two MEPs for addition to the CH end and the distance between the H atom and the CH carbon. The largest of these

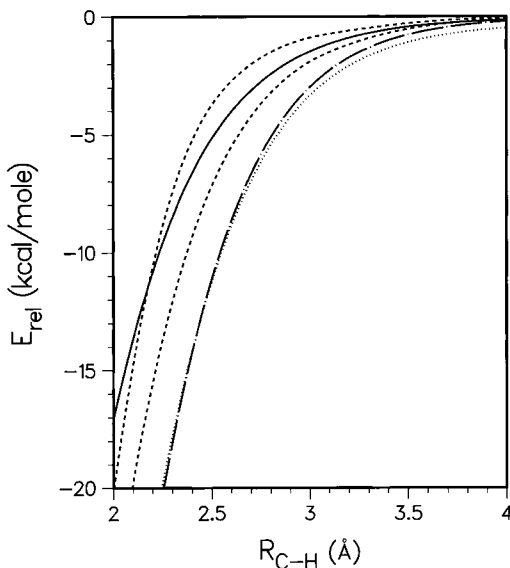


FIG. 3. MEP energies for the reactions: $\text{H} + \text{C}_3\text{H}_5 \rightarrow \text{C}_3\text{H}_6$ (solid), $\text{H} + \text{C}_3\text{H}_3 \rightarrow \text{CH}_2\text{CCH}_2$ (upper, dashed), $\text{H} + \text{C}_3\text{H}_3 \rightarrow \text{CH}_3\text{CCH}$ (lower, dashed), $\text{H} + \text{C}_2\text{H}_3 \rightarrow \text{C}_2\text{H}_4$ (dash-dot), and $\text{H} + \text{C}_2\text{H}_5 \rightarrow \text{C}_2\text{H}_6$ (dot).

two corrections was then used to correct the cc-pvdz surface at that point.

Transition State Theory

For barrierless reactions such as the radical-radical recombination reactions of interest here, the optimal form for the transition state dividing surface varies considerably with energy (E) and with total angular momentum (J). At low E and low J , the transition state lies at large interfragment separations, and the optimal reaction coordinate is simply the separation between the centers of mass of the two radicals. At higher E and/or J , the transition state moves in to shorter separations where the optimal transition state dividing surface correlates, at least qualitatively, with a fixed separation between the centers of the two orbitals involved in the incipient bond.

In this work, both the definition and location of the transition state dividing surface were variationally optimized within the set of surfaces defined by a fixed separation between the H atom and a pivot point connected to the propargyl or allyl radical. Choosing the pivot point as the center of mass of the radical yielded a form appropriate for low E and J . Alternatively, choosing the pivot point along the axis of one of the lone pair orbitals of the radical provided a dividing surface that was appropriate for high E and/or high J . Minimization of the transition state partition function with respect to both the location

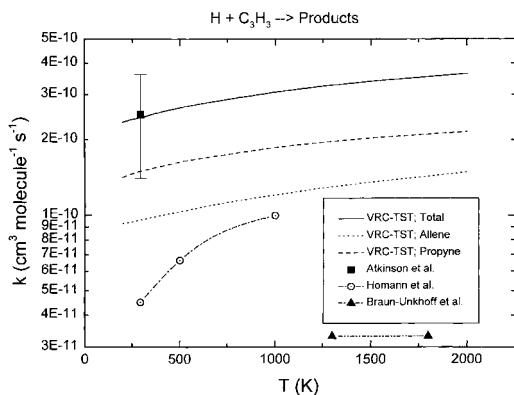


FIG. 4. Plot of the high-pressure recombination rate constant versus temperature for $\text{H} + \text{C}_3\text{H}_3$, including the separate contributions corresponding to the propyne and allene product channels.

of the radical pivot point and the separation between the H atom and the pivot point then provided the present variable reaction coordinate transition state theory estimate for the rate constant.

For the propargyl radical, there are four distinct reaction paths for the addition, corresponding to the addition of the H atom from either above or below the radical plane to either the CH or the CH_2 side of the radical. The presence of strongly repulsive regions separating each of these channels, and the extension of these repulsive regions out to fairly large separations, suggests that it is appropriate to optimize separate dividing surfaces for each of these channels. The CH (allene) and CH_2 (propyne) addition channels were distinguished here by the angle between the incoming H atom and the CC bond from the central C to the methylene C. Angles of greater than 90° are assumed to correlate with allene, while values of less than 90° are assumed to correlate with propyne.

A grid-based procedure was employed in the variational minimization at the E/J resolved level for each of these channels. The grid of radical fixed-point locations was defined in terms of the vector from the fixed point to the C atom of the incipient bond. This vector was taken to lie in the plane perpendicular to that of the radical, but passing through the CCC axis, and was defined in terms of its length d and angle θ relative to the CC axis. Sample calculations suggested that two distinct sets of (d, θ) should be considered. The first set was centered about (1.2, 0) and effectively yielded the center-of-mass reaction coordinate. The second set included d values ranging from 0.0 to 1.25 and angles ranging from about 70 to 110 . This second set sampled fixed points in the neighborhood of the radical orbital. The first set of fixed-point locations was coupled

with a grid of H atom to radical fixed-point separations R ranging from about 5.0 to about 3.25 Å with a 0.25 Å spacing. The second set of fixed-point locations was coupled with a grid of R ranging from about 3.0 to 1.75 Å again with a 0.25 Å spacing. The VARIFLEX software package [17] was used in evaluating the number of available states, $N_{\text{EJ}}(R, d, \theta)$ (i.e., the E/J resolved transition state partition function) for each point in this grid, and in performing the Boltzmann weighted integral over E and J of the minimum of N_{EJ} on the grid to obtain the thermal rate constant. Interestingly, the optimized dividing surfaces were again found to correlate closely with the contours of the radical orbitals [6].

For the allyl radical, there were again four distinct reaction paths, but these were now all symmetrically related. Each of these channels was again well separated by repulsive regions of the potential; thus, optimized dividing surfaces were considered for each channel separately. The procedure employed in these optimizations is closely analogous to that for the propargyl radical and is not reviewed here.

The variable reaction coordinate formalism [18] employed here also implements an assumed separation between the internal vibrational modes of the fragments, labeled the conserved modes, and the remaining transitional modes, which vary in character from the reactants to the products. Here, the properties of the conserved modes are assumed to be invariant in the process from reactants to the transition state. Then, their contribution to the transition state partition function cancels the corresponding contribution to the reactant partition function. In reality, both the vibrational frequencies and the optimal geometry will vary somewhat as the fragments approach one another. For example, the H atom(s) on the C being attacked by the incoming H atom will move away from the approaching H atom by bending out of the plane of the radical. Concomitant with this change in bending angle(s) will be a change in its vibrational frequency and other related torsional frequencies. However, such variations tend to be of only secondary importance. For example, for the frontside addition channel in the $\text{H} + \text{vinyl}$ reaction, these two effects yield a correction of only 4%. Thus such variations, which would require substantial additional computational effort, were neglected here.

Results and Discussion

The present MR-CI-based variable reaction coordinate transition state theory results for the $\text{H} + \text{propargyl}$ high-pressure recombination rate constant are plotted in Fig. 4. The ratio of the propyne to allene formation rate constants is roughly constant at 1.55 for temperatures up to 1000 K and then decreases gradually with increasing temperature,

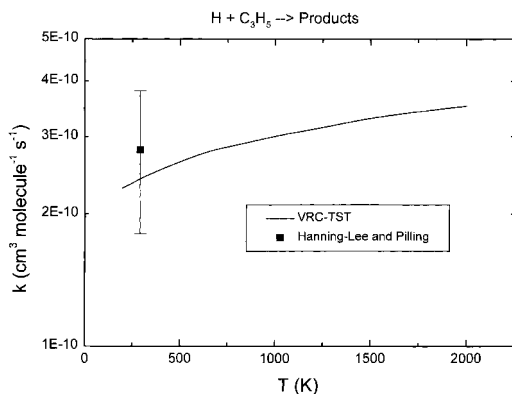


FIG. 5. Plot of the high-pressure recombination rate constant versus temperature for $\text{H} + \text{C}_3\text{H}_5$.

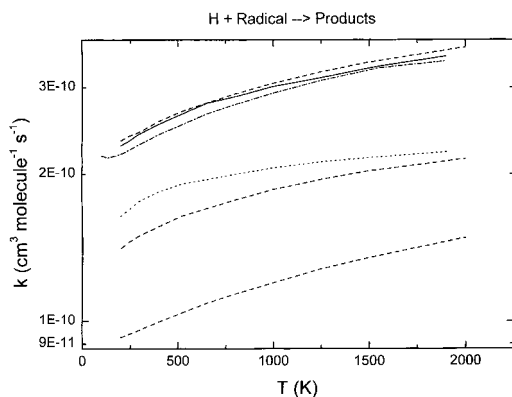


FIG. 6. Plot of the high-pressure recombination rate constant versus temperature for $\text{H} + \text{C}_3\text{H}_5$ (solid), $\text{H} + \text{C}_3\text{H}_3$ (upper, dashed), $\text{H} + \text{C}_2\text{H}_3$ (dash-dot), and $\text{H} + \text{C}_2\text{H}_5$ (dot). The two lower dashed lines are for the propyne and allene (lowest) channels of the $\text{H} + \text{C}_3\text{H}_3$ recombination.

reaching a value of 1.45 at 2000 K. This larger magnitude for the propyne formation channel is readily explained on the basis of the greater attractiveness along the MEP (cf. Fig. 3), and somewhat larger range of angles for which the interaction is attractive for this channel (cf. Fig. 1).

The available experimental results, which are indirectly determined from kinetic modeling of the pyrolysis of toluene [3], and the oxidations of acetylene [2] and propargyl [4], also are plotted in Fig. 4. The theoretical predictions are in quantitative agreement with the most recent of these experimental results, which were obtained for 6.65 mbar at 295 K. Sample master equation simulations of the pressure dependence suggest that the discrepancy of a factor of 3 to 10 with the other experimental results may be due, at least in part, to a deviation from the high-pressure limit in these experimental studies.

The present data also could be used to predict CH dissociation rates in allene and propyne, for which there is a substantially larger body of experimental data [19]. However, as has been well described by Kiefer et al. [19], the proper modeling of the dissociation process requires a good description of the effect of vibrational anharmonicities on the state density of the complex, which is beyond the scope of the present work. Our own sample master equation calculations employing the present VRC-TST model for the transition state yielded similar results to those of Ref. [19]. Thus, we do not pursue here a comparison with dissociation rates.

Related calculations of the $\text{H} + \text{C}_3\text{H}_3$ recombination rate, employing a potential which does not include the cc-pvtz basis set corrections, yielded results that were only 9% to 19% lower. Similarly, the neglect of the Davidson correction yielded results that were only 8% to 20% lower. The smallness of these two corrections suggests that any inaccuracies in the underlying potential are likely to be of only minor significance.

The present results for the $\text{H} +$ allyl recombination rate are plotted in Fig. 5. The theoretical predictions are in quantitative agreement with the fairly direct experimental measurement of Hanning-Lee and Pilling [5]. The predicted rise by a factor of 1.54 from 200 to 2000 K is identical to that predicted for the $\text{H} +$ propargyl reaction. A cc-pvtz calculation of the MEP was not performed for this reaction. However, the near constancy of the effect of this correction on the rates for a variety of reactions led us to simply incorporate a 15% increase to the rates. The effect of the Davidson correction is also expected to be similar to that for the $\text{H} +$ propargyl reaction.

A plot of the VRC-TST predictions for the high-pressure recombination rate constants for the $\text{H} +$ propargyl, allyl, vinyl and ethyl reactions is provided in Fig. 6. The rate constant for the $\text{H} + \text{C}_3\text{H}_5$ recombination is remarkably similar to the total recombination rate constant for $\text{H} + \text{C}_3\text{H}_3$. Interestingly, the $\text{H} + \text{C}_3\text{H}_5$ MEP lies roughly midway between the MEPs for the two $\text{H} + \text{C}_3\text{H}_3$ channels. As a result, while the addition to the CH_2 side of propargyl occurs at a greater rate than does the addition to one side of allyl, the addition to the CH side of propargyl occurs at a lower rate. The sum of the rates for the two propargyl channels then adds to be essentially identical to the total allyl rate.

The H-atom recombination rates for the two resonantly stabilized radicals were actually predicted to be greater than those for the vinyl and ethyl radicals. At first glance this seems to contradict the increased attractiveness for the MEPs in the vinyl and ethyl radicals (cf. Fig. 3). However, this result is simply an indication that there are essentially four separate addition channels for each of the resonantly stabilized channels, while there are only two (frontside and backside additions) for the vinyl and ethyl radicals.

TABLE I
Modified Arrhenius parameters for H + radical high pressure recombination rates

Reaction	A (10^{-11} $\text{cm}^3 \text{s}^{-1}$)	n	E_a (K)
H + C ₃ H ₅ → products	5.804	0.2363	-25.90
H + C ₃ H ₃ → products	4.520	0.2711	-42.24
H + C ₃ H ₃ → propyne	3.710	0.2298	-24.26
H + C ₃ H ₃ → allene	1.139	0.3320	-69.06
H + C ₂ H ₃ → products	4.279	0.2724	-37.56
H + C ₂ H ₅ → products	10.38	0.1017	15.84

After division by two, the rates for the allyl and propargyl radicals were, as expected, significantly smaller than those for the vinyl and ethyl radicals.

Summary

The H + allyl and H + propargyl recombination reactions were studied with variable reaction coordinate transition state theory employing interaction potentials obtained from multireference configuration interaction calculations. The predictions for the high pressure limit recombination rates were found to be essentially identical for these two reactions. The results for the H + allyl reaction were in good agreement with the only experimental study, while those for the H + propargyl reaction agreed only with those from the most recent experimental study, being considerably greater than other earlier studies. The addition to the CH₂ side of the propargyl radical was predicted to occur with a rate that is 1.5 times that for the CH side.

Table I provides the parameters A, n, and E_a from modified Arrhenius fits [$k = A T^n \exp(-E_a/T)$] to the high-pressure recombination rates for H + allyl, H + propargyl, H + vinyl, and H + ethyl. Contrary to initial expectations, the high-pressure recombination rates for the two resonantly stabilized radicals studied here were actually greater than those for the H + vinyl and H + ethyl reactions, due to the presence of twice as many addition channels for the resonantly stabilized radicals. Similar findings might be expected for the relative recombination rates with other addition partners.

The observation of elevated concentrations of these radicals thus appears to be simply the result of greater rates of formation; that is, their stabilization energy should correlate with decreased production thresholds relative to other related channels. At lower pressures these decreased production thresholds might also affect the ordering of various effective recombination rates. In particular, the redissociation of the addition products back to reactants would be expected to be greater for the resonantly

stabilized radicals due to their lower binding energy, and thus the effective loss rates would be smaller. Of course, such a pressure-dependent effect would also depend quite strongly on the lifetime (and, correspondingly, the size) of the complex.

Acknowledgments

This research was supported by the U.S. Department of Energy, Office of Basic Energy Sciences, Division of Chemical Sciences, under Contracts W-31-109-ENG-38 (LBH) and DE-FG-02-98ER14902 (SJK).

REFERENCES

1. Miller, J. A., and Melius, C. F., *Combust. Flame* 91:21-39 (1992).
2. Homann, K. H., and Wellmann, Ch., *Ber. Bunsen-Ges. Phys. Chem.* 87:609-616 (1983); and references cited therein.
3. Braun-Unkloff, M., Frank, P., and Just, Th., *Proc. Combust. Inst.* 21:1053-1061 (1988).
4. Atkinson, D. B., and Hudgens, J. W., *J. Phys. Chem. A* 103:4242-4252 (1999).
5. Hanning-Lee, M. A., and Pilling, M. J., *Int. J. Chem. Kinet.* 24:271-278 (1992).
6. Klippenstein, S. J., and Harding, L. B., *Phys. Chem. Chem. Phys.* 1:989-997 (1999).
7. Harding, L. B., and Klippenstein, S. J., *Proc. Combust. Inst.* 27:151-157 (1998).
8. Dunning Jr., T. H., *J. Chem. Phys.* 90:1007-1023 (1989).
9. Kendall, R. A., Dunning Jr., T. H., and Harrison, R. J., *J. Chem. Phys.* 96:6796-6806 (1992).
10. Woon, D. E., and Dunning Jr., T. H., *J. Chem. Phys.* 98:1358-1371 (1993).
11. Shepard, R., Shavitt, I., Pitzer, R. M., Comeau, D. C., Pepper, M., Lischka, H., Szalay, P. G., Ahlrichs, R., Brown, F. B., and Zhao, J.-G., *Int. J. Quantum Chem.* S22:149-165 (1988).
12. MOLPRO is a package of *ab initio* programs written by Werner, H.-J., and Knowles, P. J., with contributions from Almlof, J., Amos, R. D., Berning, A., Cooper, D. L., Deegan, M. J. O., Dobbyn, A. J., Eckert, F., Elbert, S. T., Hampel, C., Lindh, R., Lloyd, A. W., Meyer, W., Nicklass, A., Peterson, K., Pitzer, R., Stone, A. J., Taylor, P. R., Mura, M. E., Pulay, P., Schutz, M., Stoll, H., and Thorsteinsson, T.
13. Werner, H.-J., and Knowles, P. J., *J. Chem. Phys.* 82:5053-5063 (1985).
14. Knowles, P. J., and Werner, H.-J., *Chem. Phys. Lett.* 115:259-267 (1985).
15. Werner, H.-J., and Knowles, P. J., *J. Chem. Phys.* 89:5803-5814 (1988).
16. Knowles, P. J., and Werner, H.-J., *Chem. Phys. Lett.* 145:514-522 (1988).
17. Klippenstein, S. J., Wagner, A. F., Dunbar, R. C.,

- Wardlaw, D. M., and Robertson, S. H., *VARIFLEX, Version 1.0* (1999).
18. Klippenstein, S. J., *J. Phys. Chem.* 98:11459–11464 (1994).
19. Kiefer, J. H., Mudipalli, P. S., Sidhu, S. S., Kern, R. D., Jursic, B. S., Xie, K., and Chen, H., *J. Phys. Chem. A* 101:4057–4071 (1997); and references cited therein.

COMMENTS

Alexander Fridman, University of Illinois at Chicago, USA. The theoretical modeling presented shows an essential positive activation energy of the hydrogen-propargyl H + C₃H₃ recombination. Recent experiments give no activation energy, actually no temperature dependence at all for the reaction. Generally similar recombination processes have no essential positive activation energies. Probably, such a discrepancy is due to approximate nature of the approach.

Author's Reply. Current experiments are probably not sufficiently accurate to resolve the question as to whether or not there is a small positive activation energy for this reaction in the high pressure limit as predicted by our calculations. Our approach does give a negative temperature dependence for other reactions where the experimental evidence for a negative temperature is stronger. See, for example, CH₃ + CH₃ [1].

REFERENCE

1. Klippenstein, S. J., and Harding, L. B., *J. Phys. Chem.* 103:9388–9398 (1999).

Jürgen Troe, University of Göttingen, Germany. The transition state theory, which you use, is an adiabatic theory, that is, it corresponds to the limiting case of adiabatic capture dynamics. We have shown, however, that high pressure combination reaction of hydrogen atoms with radicals (or other open shell species) are showing partly non-adiabatic dynamics [1,2]. I, therefore, estimate that your results for 200 K have to be reduced by about 20% and for 300 K by about 10% due to these rovibrationally non-adiabatic dynamical effects.

REFERENCES

1. Harding, L. B., Troe, J., and Ushakov, V. G., *Phys. Chem. Chem. Phys.* 2:631 (2000).
2. Maergoiz, A. I., Nikitin, E. E., Troe, J., and Ushakov, V. G., *J. Chem. Phys.* 108:5265, 9987 (1998).

Author's Reply. A statistical, rather than adiabatic, theory was used in this work. For a reaction coordinate defined by the separation of the centers-of-mass of the two reacting fragments, variational statistical theory can effectively be reduced to an adiabatic channel theory. However, for generalized reaction coordinates, such as those used here, there are kinetic couplings between the reaction coordinate

and the remaining coordinates. These couplings introduce significant conceptual differences between the statistical and adiabatic channel frameworks. The correct treatment of these couplings is an important component of the current statistical theory. Importantly, it should be possible to recover the effect of the non-adiabaticities in the center-of-mass frame via the appropriate choice of generalized reaction coordinate within a variational statistical theory framework. Thus, one cannot use the comparison of trajectory simulations with adiabatic capture theory to suggest that the present results should be reduced by 10% to 20%.

P. R. Westmoreland, University of Massachusetts, Amherst, USA. We have proposed that propargyl + propargyl combination should favor combination at the CH₂ ends, as you find for the site of H + propargyl [1]. Our simplistic model was that if 90% of the electron density was on the CH₂ carbon and 10% on the CH carbon (calculated), the probabilities of 1,5-hexadiyne:hexa-4,5-dienyne:1,2,4,5-hexatetraene would be 0.81:0.18:0.01. [Note that the hexadiyne and hexatetraene can interconvert by a Cope rearrangement.] Wouldn't your results support favoring the hexadiyne?

REFERENCE

1. Thomas, S. D., Communal, F., and Westmoreland, P. R., *Preprints of Division of Fuel Chemistry American Chemical Society* 36(4):1448 (1991).

Author's Reply. Our calculations predict the CH₂ end of propargyl is more reactive (toward hydrogen atoms) than the CH end by a ratio of 0.6:0.4. If we assume that this difference in the reactivity of the two ends of propargyl carries over directly from H + C₃H₃ to C₃H₃ + C₃H₃ then we would predict the three products you mention, 1,5 hexadiyne, hexa-4,5-dienyne and 1,2,4,5 hexatetraene, to be formed in the ratios 0.36:0.48:0.16 respectively. However, it is generally found that less reactive species will react more selectively than more reactive species. Since propargyl is certainly less reactive than a hydrogen atom, we would expect the above prediction of 36% 1,5 hexadiyne to be a lower bound. In fact, recent measurements concluded that the yield of 1,5 hexadiyne from this reaction is 60% [1].

REFERENCE

1. Fahr, A., and Nayak, A., *Int. J. Chem. Kinetics* 32:118–124 (2000).

